Editors' Suggestion | Featured in Physics

Laser-Assisted Evaporative Cooling of Anions

G. Cerchiari,[†] P. Yzombard,[‡] and A. Kellerbauer[*]
Max Planck Institute for Nuclear Physics, Saupfercheckweg 1, 69117 Heidelberg, Germany

(Received 15 May 2019; published 6 September 2019)

We report the first cooling of atomic anions by laser radiation. O^- ions confined in a linear Paul trap were cooled by selectively photodetaching the hottest particles. For this purpose, anions with the highest total energy were illuminated with a 532 nm laser at their maximal radial excursion. Using laser-particle interaction, we realized a both colder and denser ion cloud, achieving a more than threefold temperature reduction from 1.15 to 0.33 eV. Compared with the interaction with a dilute buffer gas, the energy-selective addressing and removal of anions resulted in lower final temperatures, yet acted 10 times faster and preserved twice as large a fraction of ions in the final state. An ensemble of cold negative ions affords the ability to sympathetically cool any other negative ion species, enabling or facilitating a broad range of fundamental studies from interstellar chemistry to antimatter gravity. The technique can be extended to any negative ion species that can be neutralized via photodetachment.

DOI: 10.1103/PhysRevLett.123.103201

Laser cooling, which reduces the kinetic energy of neutral or charged particles, is one of the most important experimental tools in atomic physics. It allows the cooling of particle beams or ensembles to temperatures below that of the surrounding apparatus, well below 1 K. Ultracold temperatures are a prerequisite for many groundbreaking applications, such as ultraprecise clocks [1], quantum information [2], quantum computation [3], or the study of matter waves with Bose-Einstein condensates [4,5]. In the case of charged particles, laser cooling enables the formation of Coulomb crystals, regularly ordered structures that form when the electrostatic interaction prevails over thermal motion [6]. One interesting application of laser-cooled ultracold ions is the sympathetic cooling of another particle species. For instance, highly charged $^{40}Ar^{13+}$ ions have been cooled into an ordered crystalline structure suitable for precision spectroscopy by interacting with Be^+ ions at mK temperatures [7]. Other state-of-the-art experiments have combined trapped ions with a magneto-optical trap in such a way that the laser-cooled neutral atoms constitute a buffer medium which cools the trapped ions by collisions [8,9].

In negative ions, the electronic binding is characterized by a short-range potential instead of the infinite-range Coulomb potential. Because of their fragile nature, the laser cooling of negative ions has not yet been achieved. Laser-cooled anions would open the field of ultraprecision studies to a new kind of system. Furthermore, they could be used to sympathetically cool any other negatively charged particles [10]. In the case of antimatter, a neutral buffer medium cannot be used for cooling due to the risk of annihilation, whereas the repelling electric charge of anions would prevent them from annihilating with antiprotons. In this way, a sample of ultracold antiprotons could be prepared by collisions with laser-cooled negative ions. Antihydrogen subsequently formed with these antiprotons would have almost the same low temperature due to the large mass ratio of antiproton to positron. This antihydrogen production technique would open the way for a variety of high-precision antimatter experiments. For instance, a beam of antihydrogen at $\approx$100 mK is a prerequisite for an antimatter gravity measurement to test the weak equivalence principle using a moiré deflectometer [11].

Because of the weak binding of the valence electron, only very few atomic [12,13] or molecular [14,15] anions are amenable to laser cooling. Recently, La^- has been identified as the most promising atomic-anion candidate to date [16,17]. The potential Doppler cooling transition has been fully characterized [18,19]. The existence of a dark state, as well as photodetachment of the excited La^- by the cooling laser, imposes an upper limit of 100 K on the initial temperature. Starting from that temperature, an ensemble of La^- ions could be cooled to the Doppler temperature $T_D = 0.17\ \mu$K within a few seconds. When ions are loaded into an ion trap, they typically have temperatures of several 10 000 K. In order to precool them to the starting temperature for Doppler cooling, we have implemented a scheme based on the selective laser photodetachment of the hottest trapped particles, as suggested almost 30 years ago [20]. This technique is a variant of evaporative cooling, which is a well-established cooling mechanism for atoms [21] and, to a lesser extent, ions [22]. Evaporative cooling by photodetachment is only applicable to (atomic or molecular) *anions*, because neither cations nor negative subatomic particles can be removed from an ion trap by photodetachment. In this Letter we report the successful cooling of O^- ions with this technique, employing geometrical selection.

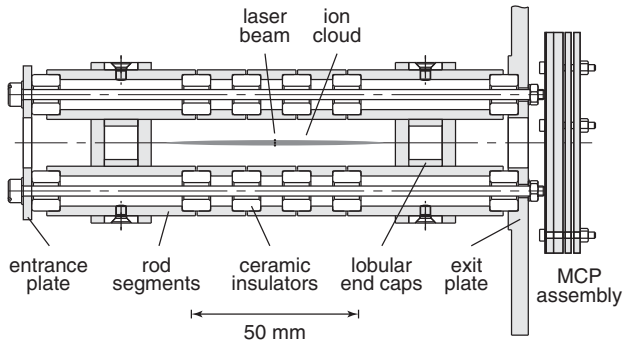

FIG. 1. Schematic drawing of the linear Paul trap. Ions enter the trap from the left and exit towards the MCP detector to the right.

This is the first demonstration of the direct cooling of a negative ion species using optical radiation.

The experiments reported here were carried out with O^- ions [electron affinity $E_A = 1.4611136(9)$ eV [23], using the most recent conversion factor from m^{-1} to eV [24]] confined in a linear Paul trap. The trap, the trapping method, as well as the detection technique are described in detail in Ref. [25]. Briefly, the linear trap is composed of four cylindrical parallel electrodes (rods). A cross-sectional view is shown in Fig. 1. The rods have a diameter of 14.8 mm and a distance between the trap axis and the inner electrode surface of $r_0 = 7$ mm. A radio frequency (rf) signal is applied to one pair of opposing rods, whereas the signal on the second pair of rods has a phase shift of π. The applied rf has a frequency of $\Omega_{\mathrm{rf}}/(2\pi) = 1.938$ MHz and an amplitude (peak to peak) of $V_{pp} = 225(20)$ V. The amplitude was chosen for optimal ion loading. Additional electrodes (lobe-shaped end caps) provide axial ion confinement in a region of 65(5) mm length. Photodetachment of the anions is achieved by the light of a 532 nm laser ($h\nu = 2.33$ eV) focused on the trap region.

The trap is loaded by allowing an ion beam with current ≈800 pA to pass through the trap for 100 s while the longitudinal trap potentials are in loading configuration. After the loading phase, the trap is closed by raising the potential of the downstream end cap and the system is left to evolve for 10 s until it reaches equilibrium. This settling time agrees with typical thermalization rates of ≈1–5 s encountered in ion-ion Coulomb collisions [26,27]. In this way, reproducible initial conditions for the ensuing experiments are established. After the loading process, $(1.5–2.0) \times 10^4$ anions with an average density of $(3–5) \times 10^4$ cm^{-3} are typically confined in the trap. The ion cloud is strongly elongated along the axis with a typical aspect ratio of 1:40. Most of the anions are O^- and a small fraction (< 10%) are composed of contaminants. These particles with a mass of 28–39 u could not be clearly identified [25], but remain in the trap over very long times and are unaffected by the green laser light. These background ions are apparently less prone to recombination with residual gas due to their higher electron affinity.

The number N of trapped anions and their temperature k_BT are recorded destructively. At the end of each trial, the trap is opened by switching the downstream end cap to the rod potential. The trapped particles are then free to move towards a microchannel plate (MCP) detector located at a distance of ≈5 mm from the exit plate of the trap. The MCP is equipped with a phosphor screen that converts the amplified current of secondary electrons into light, which in turn is recorded with a digital camera. The MCP image is an axial projection of the ejected ion cloud. The radially confining pseudopotential has approximately cylindrical symmetry near the axis, whereas for large excursions the radial potential becomes slightly asymmetrical. The axial confinement can be considered a simple box potential. Assuming thermal equilibrium, anions arrange in the trap according to the Boltzmann distribution. Furthermore, in the approximation of a harmonic radial potential, the average values of the kinetic and potential energies are equal (equipartition) [20].

Thus, the radial temperature can be extracted by fitting the density function $p(r) \propto \exp(-r^2/\sigma^2)$ to the radial intensity of the images. The spatial width σ of the anion cloud is related to the temperature of the ions by the expression $\sigma = \sqrt{k_BT/(m\omega^2)}$, where k_B is the Boltzmann constant and ω is the angular frequency of the anions' radial oscillations in the trap. The latter can be approximated by $\omega = \sqrt{2}eV_{pp}/(2m\Omega_{\mathrm{rf}}r_0^2)$, where m is the anion mass [28]. The systematic uncertainty of the radial position was estimated by a Monte Carlo simulation to be of the order of 10%. This uncertainty and that of V_{pp} affect all acquisitions similarly. Therefore, these systematic uncertainties are omitted in all graphs. The axial ejection was not locked to the rf phase, and no dependence of the measured ion temperature on this (arbitrary) phase was observed.

The laser beam with a Gaussian radial profile is focused into the trap region using a biconvex lens with focal length 300 mm located 294(1) mm from the focus. The position of the laser beam inside the trap is adjusted by displacing the lens in the plane perpendicular to the light propagation. In a Cartesian reference frame (x, y, z), where the trap is aligned with the z axis and the laser light propagates in the y direction, the expression for the laser beam intensity I as a function of the x coordinate is thus

$$I(x) = \frac{I_0}{\sqrt{\pi}w}\exp\left(\frac{(x-d)^2+z^2}{w^2}\right), \qquad (1)$$

where $w = 0.35(25)$ mm is the diameter of the beam waist and d is the displacement of the laser beam in the x direction.

The pressure in the experiment chamber is about 5×10^{-10} mbar. Because of collisions of anions with residual gas, we observe both a buffer-gas cooling effect with a final temperature $k_BT \approx 0.75$ eV and a limited lifetime (< 2 min). In order to achieve more efficient cooling, the most energetic anions should be removed

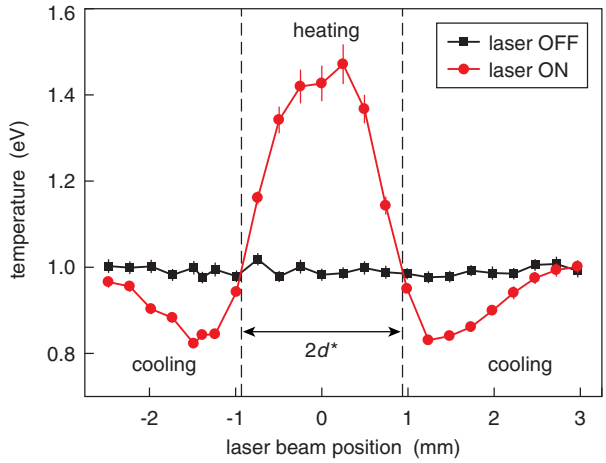

FIG. 2. Final anion temperature as a function of the lens (and hence laser beam) displacement from the trap axis after 12 s of laser illumination. Vertical dashed lines indicate the lens positions at which neither ion heating nor cooling occurs.

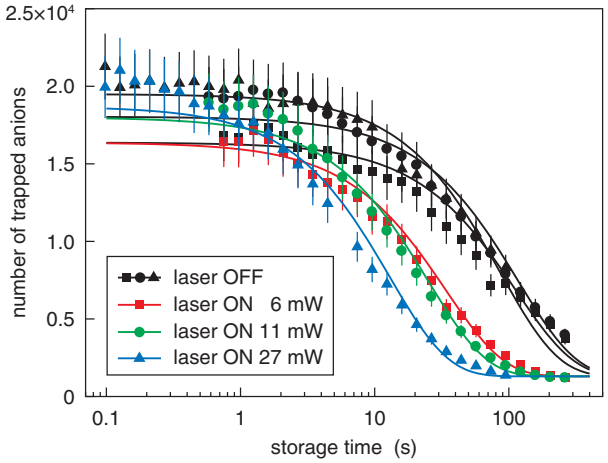

FIG. 3. Number of O^- ions in the trap as a function of storage time. The measurements with the laser on were acquired with the laser beam positioned at $d = 1.5$ mm [Eq. (1)]. Datasets with laser on and off denoted with the same symbols were taken contemporaneously under otherwise identical conditions. Solid lines are fits to the data using the function of Eq. (2).

from the trap. Those particles with the highest total energy are also those with the highest radial amplitude at their maximal radial excursion. By adjusting the displacement d of the laser beam waist from the axis, it is possible to heat or cool the ion ensemble by selectively interacting with anions orbiting close to or far from the trap axis. If d^* denotes the laser displacement for which neither a net cooling nor a net heating effect is achieved, setting the average energy of the illuminated anions equal to the total average energy per anion in the trap, we obtain the expression $d^* = \sqrt{(w^2 + \sigma^2)/2}$, which will be used to support the interpretation of our experimental results.

We performed three sets of measurements to demonstrate cooling by selective photodetachment. In all cases, the ion evolution with and without the laser radiation interacting with the anions was recorded for the same time duration. In this way, it was possible to directly compare the evolution of the system with and without laser interaction.

We first varied the displacement d of the laser beam from the trap axis by adjusting the position of the focusing lens. The laser shutter was opened for 12 s at a laser power of 11 mW. Figure 2 shows a comparison of the final temperatures obtained with and without illumination. A temperature reduction is observed if ions with large oscillation amplitudes are photodetached, while the ensemble is *heated* if ions closer to the trap axis are removed. The laser beam displacement d^*, the position where neither cooling nor heating occurs, corresponds to the crossover points of the two datasets shown in the figure. The value $d^*_{\text{expt}} = 0.93(5)$ mm compares well with the calculated value $d^*_{\text{theo}} = 1.10(15)$ mm, thus supporting the explanation of the cooling mechanism.

We then positioned the laser beam to remove anions at a distance $d = 1.5$ mm from the trap axis (minima of the red line in Fig. 2, maximum cooling) and measured the storage time as a function of the laser power from 6 to 27 mW.

Figure 3 shows that, as expected, the lifetime of the anions decreases due to photodetachment. The decrease in the number of ions was modeled with an exponential decay law with a constant fraction $N_{\text{cont}} = 1.3 \times 10^3$ to account for contaminant ions that resist photodetachment:

$$N = N_0 \exp\left(-\frac{t}{\tau}\right) + N_{\text{cont}}. \tag{2}$$

The fit results of the ion lifetimes are indicated in Table I.

As mentioned above, the ion temperature of the trapped anions decreases even without laser irradiation, due to cooling by collisions and thermalization with residual gas. However, Fig. 4 shows that the cooling rate is strongly enhanced by the detachment laser. The thermalization curve was fitted with the following expression:

$$T = (T_0 - T_\infty) \exp\left(-\frac{t}{\theta}\right) + T_\infty, \tag{3}$$

TABLE I. Lifetime parameters extracted using Eq. (2) with and without laser illumination. Grouped data sets were taken under similar conditions.

Laser power	$N_0 \times 10^{-4}$	τ (s)
Off	1.51(5)	113(7)
6 mW	1.51(4)	34(1)
Off	1.67(4)	117(6)
11 mW	1.67(4)	25.1(9)
Off	1.82(2)	86(4)
27 mW	1.74(5)	13.0(6)

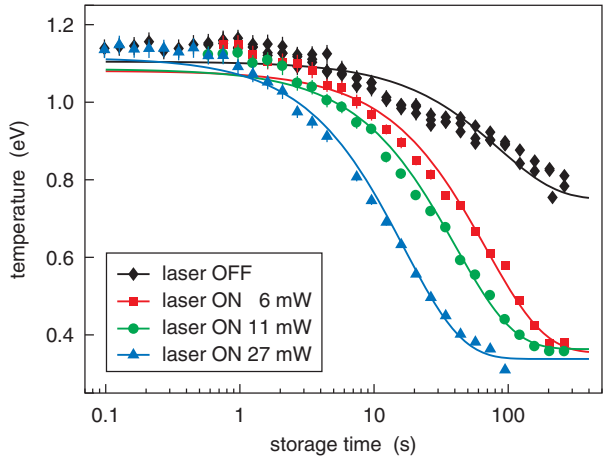

FIG. 4. Temperature of O^- anions in the trap as a function of storage time. The measurements with the laser were acquired with $d = 1.5$ mm [Eq. (1)]. Solid lines are fits to the data using the function of Eq. (3).

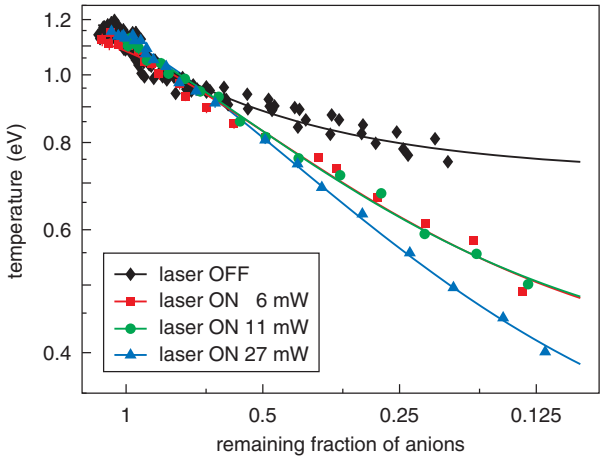

FIG. 5. Anion temperature as a function of the fraction of ions remaining in the trap. The number of remaining anions is normalized to the initial population before cooling. Error bars are comparable to the size of the data points. Solid lines are second-order polynomial fits and are meant to guide the eye.

where T_0 is the starting temperature, T_∞ is the asymptotic final temperature, and θ is the characteristic cooling time. The parameters obtained from the fits are given in Table II. The cooling rate θ is enhanced in the presence of the laser light, and more so for higher laser powers. Most importantly, the asymptotic final temperature T_∞ is also significantly lower with the laser on (≈0.35 eV) than without laser (≈0.75 eV).

Adopting this cooling scheme, it was possible to prepare a larger ensemble of anions at a lower temperature than without laser excitation. To highlight this effect, Fig. 5 shows the ion temperature as a function of the fraction of anions remaining in the trap after cooling. For instance, when 3/4 of the anions have been removed or lost, a temperature of 0.56(17) eV is obtained by cooling at 27 mW laser power, compared to 0.80(24) eV with the laser off. To reach this condition the laser interacted with the ions for < 20 s, whereas a similar ion loss took more than 10 times longer without laser due to the lower loss rate with only collisional detachment.

Finally, we monitored the temperature of the stored anions after a brief laser-induced cooling cycle. The system was prepared in a similar condition as previously, with the laser beam position fixed at $d = 1.5$ mm. After selective photodetachment during 12 s at a laser power of 11 mW, the ion cloud was allowed to evolve freely in the trap. The result is shown in Fig. 6, where the ion temperature is plotted as a function of the additional storage time after cooling. The figure shows that the temperature reduction induced by the selective laser photodetachment persists quasi-indefinitely. This indicates that after evaporative cooling the entire anion cloud reaches thermal equilibrium, as expected. While the data show that a similar final temperature is also reached without selective photodetachment (at this low laser power), it is evident from Fig. 3 that the remaining fraction of ions is much smaller after 120 s of storage time without laser (≈25%) than after 12 s of cooling (≈75%).

TABLE II. Starting temperature, asymptotic final temperature, and cooling time obtained from the fit of Eq. (2) to the data of Fig. 4.

Laser power	T_0 (eV)	T_∞ (eV)	θ (s)
Off	1.105(7)	0.75[a]	85(5)
6 mW	1.08(2)	0.35(1)	69(4)
11 mW	1.09(1)	0.363(7)	40(2)
27 mW	1.12(2)	0.338(7)	16.8(7)

[a]Parameter obtained from fit of Fig. 5 and held fixed for this fit.

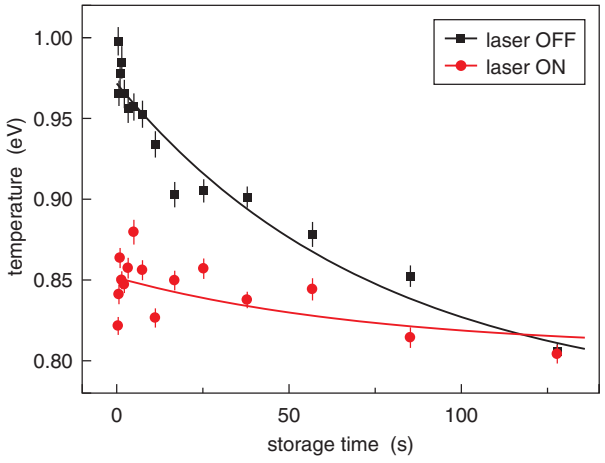

FIG. 6. Anion temperature as a function of storage time after the end of laser-induced cooling. Solid lines are simple exponential fits to the data.

In summary, we have presented the first cooling of trapped negative ions induced by a light field. Laser light is used to selectively remove the hottest particles by photodetachment. The selection is applied by geometrically addressing those anions with the largest radial oscillation amplitude. In this way, the ions' temperature was reduced from 1.15 eV (13 000 K) to 0.33 eV (3800 K) within about 100 s. With this technique the stored anions can be cooled faster and to lower temperatures than can be achieved by buffer-gas cooling with residual gas. For instance, we observed a more than twofold improvement in the limiting final temperature, and that temperature can be reached about 10 times faster than by buffer-gas cooling alone.

The technique can easily be extended to other negative ion species, assuming a laser is available that can photodetach them directly. State-of-the-art lasers for this task are generally available, as typical electron affinities are of the order of 1 eV. Heavier anions up to ^{139}La can be confined in our Paul trap with a rf drive amplitude of 1.9–2.0 kV (peak to peak), or at a correspondingly lower amplitude in a trap with smaller radial dimensions. Faster cooling can be realized by illuminating ions over a broader axial region and by compressing the ion cloud in the axial direction to enhance overlap and ion-ion collision rate. Displacing the laser position radially inward during cooling could help optimize the cooling rate and decrease ion losses. Finally, the cooling scheme could be combined with an additional resonant excitation step, which would allow the laser to be red detuned for Doppler selection of the hottest particles. This would enhance both the selectivity and the efficiency of the overall cooling process.

The authors thank the MPIK mechanical workshop for their excellent work in constructing the linear rf trap. This work was supported by the European Research Council (ERC) under Grant No. 259209 (UNIC).

*Corresponding author.
a.kellerbauer@cern.ch
†Present address: Institut für Experimentalphysik, Universität Innsbruck, Technikerstr. 25, 6020 Innsbruck, Austria.
‡Present address: Centre for Cold Matter, Blackett Laboratory, Imperial College London, Prince Consort Road, London SW7 2AZ, United Kingdom.

[1] J.-S. Chen, S. M. Brewer, C. W. Chou, D. J. Wineland, D. R. Leibrandt, and D. B. Hume, Phys. Rev. Lett. **118**, 053002 (2017).
[2] W. Rosenfeld, D. Burchardt, R. Garthoff, K. Redeker, N. Ortegel, M. Rau, and H. Weinfurter, Phys. Rev. Lett. **119**, 010402 (2017).
[3] N. Friis, O. Marty, C. Maier, C. Hempel, M. Holzäpfel, P. Jurcevic, M. B. Plenio, M. Huber, C. Roos, R. Blatt *et al.*, Phys. Rev. X **8**, 021012 (2018).
[4] M. H. Anderson, J. R. Ensher, M. R. Matthews, C. E. Wieman, and E. A. Cornell, Science **269**, 198 (1995).
[5] K. B. Davis, M.-O. Mewes, M. R. Andrews, N. J. van Druten, D. S. Durfee, D. M. Kurn, and W. Ketterle, Phys. Rev. Lett. **75**, 3969 (1995).
[6] M. Drewsen, Physica (Amsterdam) **460B**, 105 (2015).
[7] L. Schmöger, O. O. Versolato, M. Schwarz, M. Kohnen, A. Windberger, B. Piest, S. Feuchtenbeiner, J. Pedregosa-Gutierrez, T. Leopold, P. Micke *et al.*, Science **347**, 1233 (2015).
[8] W. G. Rellergert, S. T. Sullivan, S. J. Schowalter, S. Kotochigova, K. Chen, and E. R. Hudson, Nature (London) **495**, 490 (2013).
[9] B. Höltkemeier, P. Weckesser, H. López-Carrera, and M. Weidemüller, Phys. Rev. Lett. **116**, 233003 (2016).
[10] A. Kellerbauer and J. Walz, New J. Phys. **8**, 45 (2006).
[11] A. Kellerbauer *et al.* (AEGIS Proto-Collaboration), Nucl. Instrum. Methods B **266**, 351 (2008).
[12] U. Warring, M. Amoretti, C. Canali, A. Fischer, R. Heyne, J. O. Meier, C. Morhard, and A. Kellerbauer, Phys. Rev. Lett. **102**, 043001 (2009).
[13] C. W. Walter, N. D. Gibson, Y.-G. Li, D. J. Matyas, R. M. Alton, S. E. Lou, R. L. Field, D. Hanstorp, L. Pan, and D. R. Beck, Phys. Rev. A **84**, 032514 (2011).
[14] P. Yzombard, M. Hamamda, S. Gerber, M. Doser, and D. Comparat, Phys. Rev. Lett. **114**, 213001 (2015).
[15] S. Gerber, J. Fesel, M. Doser, and D. Comparat, New J. Phys. **20**, 023024 (2018).
[16] S. M. O'Malley and D. R. Beck, Phys. Rev. A **81**, 032503 (2010).
[17] C. W. Walter, N. D. Gibson, D. J. Matyas, C. Crocker, K. A. Dungan, B. R. Matola, and J. Rohlén, Phys. Rev. Lett. **113**, 063001 (2014).
[18] E. Jordan, G. Cerchiari, S. Fritzsche, and A. Kellerbauer, Phys. Rev. Lett. **115**, 113001 (2015).
[19] G. Cerchiari, A. Kellerbauer, M. S. Safronova, U. I. Safronova, and P. Yzombard, Phys. Rev. Lett. **120**, 133205 (2018).
[20] A. Crubellier, J. Phys. B **23**, 3585 (1990).
[21] W. Ketterle and N. J. Van Druten, Adv. At. Mol. Opt. Phys. **37**, 181 (1996).
[22] B. M. Penetrante, J. N. Bardsley, M. A. Levine, D. A. Knapp, and R. E. Marrs, Phys. Rev. A **43**, 4873 (1991).
[23] W. Chaibi, R. J. Pelaez, C. Blondel, C. Drag, and C. Delsart, Eur. Phys. J. D **58**, 29 (2010).
[24] E. Tiesinga, P. J. Mohr, D. B. Newell, and B. N. Taylor, The 2018 CODATA Recommended Values of the Fundamental Physical Constants (Web version 8.0), National Institute of Standards and Technology, 2019, http://physics.nist.gov/constants.
[25] G. Cerchiari, S. Erlewein, P. Yzombard, M. Zimmermann, and A. Kellerbauer, J. Phys. B **52**, 155003 (2019).
[26] J. Huba, NRL Plasma Formulary, Naval Research Laboratory, Plasma Physics Division, 2018, https://www.nrl.navy.mil/ppd/sites/www.nrl.navy.mil.ppd/files/pdfs/NRL_FORMULARY_18.pdf.
[27] L. Spitzer, *Physics of Fully Ionized Gases*, 2nd ed. (Dover, New York, 2013).
[28] M. Drewsen and A. Brøner, Phys. Rev. A **62**, 045401 (2000).